

Reversible Structural Switching of a DNA–DDAB Film

Thorsten Neumann,^{†,§} Surekha Gajria,[†] Matthew Tirrell,^{‡,§} and Luc Jaeger^{*,†,§}

Department of Chemistry and Biochemistry, Department of Chemical Engineering, and Materials Research Laboratory, University of California, Santa Barbara, California 93106-9510

Received November 30, 2008; E-mail: jaeger@chem.ucsb.edu

Nucleic acid self-assembling nanostructures interfaced with other biomolecules have great potential for materials science.¹ Naturally derived polyanions such as nucleic acids can self-assemble with cationic lipids via electrostatic complexation, which is thermodynamically driven by the release of counterions.² These complexes dispersed in water have been extensively studied and recognized as useful for gene and siRNA delivery. Their structures in water are dependent on factors such as temperature and colipid ratio and often assume the forms preferred by the lipid. For example, complexes of DNA with dimethyldidodecylammonium bromide (DDAB) or dioleoylglycerophosphocholine (DOPC) tend to form lamellar structures whereas those with dilinoleoylglycerophosphoethanolamine (DOPE) form inverted hexagonal structures, while the DNA itself remains as double-stranded DNA (dsDNA).³ Certain nucleic acid–cationic lipid mixtures are water-insoluble complexes that can form self-standing films when cast from an organic solvent such as chloroform or ethanol.⁴ In a previous study, we found that the tensile and structural properties of these films can be tuned by blending RNA and DNA of different molecular weights.⁵ However, the structure of nucleic acid–lipid films and, in particular, the state of the DNA and lipid within the films have been controversial subjects. While it has been reported that the DNA within the film retains its double-stranded helical form,⁴ recent studies have suggested that the DNA in such films is single-stranded DNA (ssDNA);⁶ however, experimental evidence remains scarce, as no structure has been given to satisfactorily explain the state of the lipid. Herein, we report the structural characterization of the switching of a DNA–DDAB film, as summarized schematically in Figure 1A.

Films were prepared by mixing aqueous solutions of DNA (~2000 bp) and DDAB to form a water-insoluble complex that was purified, dried, and dissolved in 2-propanol prior to casting on a glass slide [see the Supporting Information (SI)]. Atomic force microscopy (AFM) analysis of the surface morphology shows planar surfaces separated by equal steps that are 2.85 ± 0.3 nm in height (Figure 1C and Figure S1 in the SI). The phase image indicates that the flat surfaces are hydrophobic because of an uppermost layer of lipid tails and that the sides of the steps have some hydrophilic character due to both the lipid head groups and the DNA phosphate backbone (Figure S1). Wide-angle and small-angle X-ray scattering (WAXS and SAXS, respectively) confirm that the surface morphology represents the structure of the bulk film, yielding a repeat distance of 2.85 ± 0.2 nm from the main scattering peak at 2.2 nm^{-1} . X-ray reflectivity studies of a 49 nm thick dip-coated film also indicate that each layer has a repeat distance of 2.85 ± 0.2 nm (Figure S3 in the SI). We conclude that the films in the dry state have a lamellar structure, since two peaks were observed in a harmonic series ($q_0 = 2.2 \text{ nm}^{-1}$, $q_2 = 4.4 \text{ nm}^{-1}$) (Figure S2 in the SI). However, a repeat distance of 2.85 nm does not agree with the dimensions of a model structure of dsDNA (~2 nm in diameter) and a lipid bilayer of 2.4 nm (interdigitated, according to experimental results⁷ or 3.4 nm (without interdigitation, obtained from theoretical calculations).⁸

Strikingly, WAXS studies indicate that the repeat distance of the film increases to 4.3 ± 0.2 nm ($q = 1.48 \text{ nm}^{-1}$) when the film is immersed in water (Figure 1D). As we previously reported,⁵ this

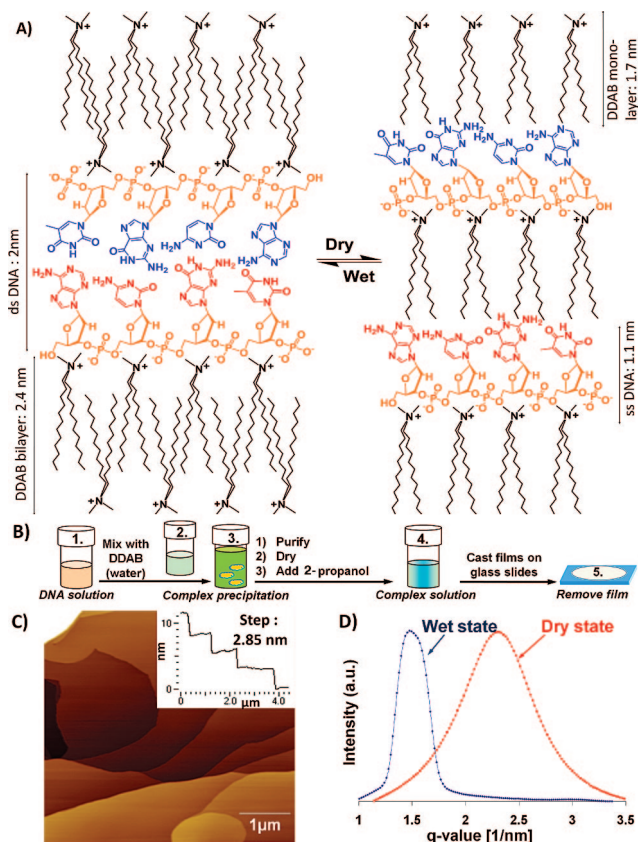


Figure 1. (A) Model for the film structure in the (left) wet and (right) dry states. (B) Procedure for preparing DNA–DDAB films (see the SI): (1) native DNA (~2000 bp), dissolved in buffer (TBE, pH 8.5) and heated at 90 °C prior to renaturation at 20 °C, is mixed with DDAB in water (2) to form an insoluble complex (3); after being purified, dried, and dissolved in 2-propanol (4), the complex is cast on a glass slide to form a dry, self-standing film (5). (C) AFM image of the surface of a DNA–DDAB film in the dry state. (D) WAXS/SAXS data for films in the dry and wet states.

corresponds to a layer of dsDNA and an interdigitated bilayer of DDAB (Figure 1A, left). This structural change can be repeatedly reversed by drying the film. At a macroscopic level, a 155% increase in the cubic volume is observed when a thick film is immersed in water (data not shown). This swelling ratio is directly correlated to the percent difference in the repeat distances in the dry and wet states at the nanoscopic level.

Our scattering data suggest that the film in the dry state has a lamellar structure formed by the repeat of an ~1.1 nm thick ssDNA layer⁹ that interacts with an ~1.7 nm thick lipid monolayer corresponding to DDAB molecules with fully extended tails⁸ (Figure 1A, right). As ssDNA is more hydrophobic than dsDNA,¹⁰ its base moieties can interact hydrophobically with DDAB lipid tails and its phosphate groups electrostatically complex with the cationic head groups of DDAB.

The DNA structures in the dry and wet films were further examined by FT-IR spectroscopy to analyze the interactions of the

[†] Department of Chemistry and Biochemistry.

[§] Materials Research Laboratory.

[‡] Department of Chemical Engineering.

DNA bases, phosphate backbone, and DDAB (Figure 2A). From the literature, it is known that both dsDNA and ssDNA have absorbance bands at 1652 and 1691 cm^{-1} that correspond to the in-plane base vibrations, particularly the carbonyl stretches of thymine and guanine. The band at 1691 cm^{-1} arises from the C6 carbonyl stretch of base-paired guanine and the C2 carbonyl stretch of paired thymine, while the band at 1658 cm^{-1} arises from the C6 carbonyl stretching vibrations of unpaired guanine, the C2 carbonyl stretches of unpaired cytosine, and the C4 carbonyl stretches of unpaired thymine. These peaks can then be used to determine whether hydrogen bonding is present. Our measurements on native dsDNA are comparable with surface-based measurements from the literature and show a stronger absorption at 1652 cm^{-1} than at 1691 cm^{-1} , while ssDNA shows the opposite: a stronger absorption at 1693 cm^{-1} and a weaker one at 1652 cm^{-1} .¹¹ In the dry state, the DNA–DDAB film exhibits a stronger absorption at 1691 cm^{-1} , with peaks similar to those of ssDNA (Figure 2C). In contrast, the film immersed in water has characteristics similar to those of B-form dsDNA in this region. The conversion of ssDNA into dsDNA can be monitored by FT-IR and occurs on the order of minutes (Figure S4 in the SI). Circular dichroism (CD) spectra of the dry and wet films give further evidence that the DNA is essentially single-stranded (nonhelical) and double-stranded (helical) in the dry and wet films, respectively (Figure S5 in the SI). In agreement with the FT-IR and SAXS studies, intercalation studies with ethidium bromide-treated DNA–DDAB films corroborate the dsDNA-to-ssDNA transition when wet films are dried (data not shown).

The lipid also undergoes a structural change from bilayer to monolayer as the film is dried. Evidence for this change can be seen in the IR absorbance bands for the symmetric stretching of CH_2 groups at 2852 cm^{-1} (ν_s) and the asymmetric stretches at 2923 cm^{-1} (ν_{as}) (Figure 2B).¹² Both the DDAB and DNA–DDAB films in water show a local maximum at 2923 cm^{-1} , while the dry film shows a shifted band at 2927 cm^{-1} . The position of the absorption band at 2852 cm^{-1} is independent of the treatment of the DNA–DDAB film. The intensity ratio for the 2852 and 2923 cm^{-1} peaks is 1:0.09 for the dry DNA–DDAB film, while for the wet film as well as for DDAB alone, it is in the range of 1:0.5 to 1:0.6. A stronger intensity in ν_{as} indicates a smaller amount of interdigitated lipid (i.e., a lipid monolayer).

The melting point of the DNA duplex decreases when organic solvents or long alkyl chains (e.g., in a reversed-phase column) lower the base-stacking energy through hydrophobic/hydrophobic interactions.¹³ Similarly, at a low water content, DDAB molecules interact with the bases and favor the dsDNA-to-ssDNA transition. In contrast, when the film is immersed in water, the hydrophilic interactions between the DNA and water molecules might favor the ssDNA-to-dsDNA transition.

In conclusion, DNA–DDAB films undergo a reversible structural transition from double- to single-stranded and from bilayer to monolayer as the water content in the film decreases. Our models for the film in the dry and wet states suggest that one of the two DNA strands and the DDAB molecules switch positions when the film dries (Figure 1A). This means that the lipid bilayer, which can be described as interdigitated alkyl chains, is disrupted, and a monolayer of lipids is formed. The hydrophilic headgroup of the lipid monolayer interacts with the phosphate backbone of the DNA while the lipid alkyl chains interact with the bases of the ssDNA. This local switching could also explain why the two single strands of the DNA in the dry film are able to find their complementary partners quickly when the film is immersed in water. The presence of water is thus essential for maintaining the stability of the DNA double helix.

Because of this phenomenon and the interplay of nucleic acid self-assembly and lipid self-organization, DNA–lipid films are interesting models for the design of new responsive materials with

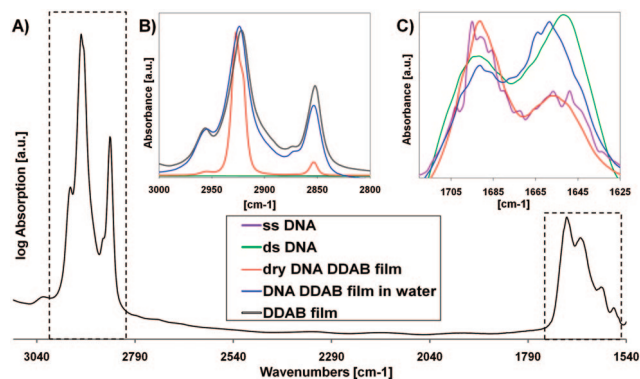


Figure 2. (A) Full FT-IR spectrum of the DNA–DDAB film in the dry state. Specific absorbance bands for (B) the lipid and (C) the DNA bases in the DNA–DDAB film in the dry and wet states and the controls of ssDNA, dsDNA, and DDAB alone.

applications in electronics, medicine, and synthetic biology (for instance, a new formulation for nucleic acid delivery).^{4–6,14}

Acknowledgment. We thank Prof. Song-I Han and Dr. Ravinath Kausik for helpful discussions and Dr. Wirasak Smithipong for initiating the project. This work was supported by the MRSEC Program of the National Science Foundation under Grants DMR05-20415 (L.J. and M.T.) and DMR-0710521 (Materials World Network) (M.T.) and the National Institutes of Health under Grant R01 GM079604-01 (L.J.).

Supporting Information Available: Experimental procedures and further characterization of the structure and switching of the films. This material is available free of charge via the Internet at <http://pubs.acs.org>.

References

- (1) (a) Seeman, N. C. *Mol. Biotechnol.* **2007**, *37*, 246. (b) Pianowski, Z. L.; Winssinger, N. *Chem. Soc. Rev.* **2008**, *37*, 1330. (c) Lu, Y.; Liu, J. *Acc. Chem. Res.* **2007**, *40*, 315. (d) Jaeger, L.; Chworos, A. *Curr. Opin. Struct. Biol.* **2006**, *16*, 531.
- (2) Rädler, J.; Koltover, I.; Salditt, T.; Safinya, C. R. *Science* **1997**, *275*, 810.
- (3) (a) Bouxsein, N. F.; McAllister, C. S.; Ewert, K. K.; Samuel, C. E.; Safinya, C. R. *Biochemistry* **2007**, *46*, 4785. (b) Gawrisch, K.; Parsegian, V. A.; Hajduk, D. A.; Tate, M. W.; Gruner, S. M.; Fuller, N. L.; Rand, R. P. *Biochemistry* **1992**, *31*, 2856.
- (4) (a) Ijro, K.; Okahata, Y. *J. Chem. Soc., Chem. Commun.* **1992**, 1339. (b) Hoshino, Y.; Tajima, S.; Nakayama, H.; Okahata, Y. *Macromol. Rapid Commun.* **2002**, *23*, 253.
- (5) Smithipong, W.; Neumann, T.; Gajria, S.; Li, Y.; Chworos, A.; Jaeger, L.; Tirrell, M. *Biomacromolecules* **2009**, *10*, 221.
- (6) (a) Cristofolini, L.; Berzina, T.; Erokhin, V.; Tenti, M.; Fontana, M. P.; Erokhin, S.; Kononov, O. *Colloids Surf., A* **2008**, *321*, 158. (b) Sukhorukov, G. B.; Feigin, L. A.; Montrel, M. M.; Sukhorukov, B. I. *Thin Solid Films* **1995**, *259*, 79.
- (7) (a) Zemb, T.; Belloni, L.; Dubois, M.; Marcelja, S. *Prog. Colloid Polym. Sci.* **1992**, *89*, 33. (b) Zemb, T.; Gazeau, D.; Dubois, M.; Gulik-Krzywicki, T. *Europhys. Lett.* **1993**, *21*, 759.
- (8) *Protein Architecture: Interfacing Molecular Assemblies and Immobilization Biotechnology*; Lvov, Y., Möhwald, H., Eds.; Marcel Dekker: New York, 2000.
- (9) Zhou, J.; Gregurick, S. K.; Krueger, S.; Schwarz, F. P. *Biophys. J.* **2006**, *90*, 544.
- (10) Costa, D.; Miguel, M. G.; Lindman, B. *J. Phys. Chem. B* **2007**, *111*, 10886.
- (11) (a) Malins, D. C.; Polissar, N. L.; Ostrander, G. K.; Vinson, M. A. *Proc. Natl. Acad. Sci. U.S.A.* **2000**, *97*, 12442. (b) Banyay, M.; Sarkar, M.; Gräslund, A. *Biophys. Chem.* **2003**, *104*, 477. (c) Brewer, S. H.; Anthireya, S. J.; Lappi, S. E.; Drapcho, D. L.; Franzen, S. *Langmuir* **2002**, *18*, 4460.
- (12) Hull, M. C. *Anal. Chem.* **2005**, *77*, 6096.
- (13) (a) Mikhailenko, I.; Shlyakhtenko, L. *J. Biomol. Struct. Dyn.* **1984**, *6*, 1501. (b) McFarland, G. D.; Borer, P. N. *Nucleic Acids Res.* **1979**, *7*, 1067.
- (14) (a) Inoue, Y.; Fukushima, T.; Hayakawa, T.; Ogura, R.; Kaminishi, H.; Miyazaki, K.; Okahata, Y. *J. Biomed. Mater. Res., Part A* **2006**, *76*, 126. (b) Fukushima, T.; Hayakawa, T.; Inoue, Y.; Miyazaki, K.; Okahata, Y. *Biomaterials* **2004**, *25*, 5491.

JA809349M